LETTERS

# Magnetic order close to superconductivity in the iron-based layered $LaO_{1-x}F_xFeAs$ systems

Clarina de la Cruz[1,2], Q. Huang[3], J. W. Lynn[3], Jiying Li[3,4], W. Ratcliff II[3], J. L. Zarestky[5], H. A. Mook[2], G. F. Chen[6], J. L. Luo[6], N. L. Wang[6] & Pengcheng Dai[1,2]

**Following the discovery of long-range antiferromagnetic order in the parent compounds of high-transition-temperature (high-$T_c$) copper oxides[1,2], there have been efforts to understand the role of magnetism in the superconductivity that occurs when mobile 'electrons' or 'holes' are doped into the antiferromagnetic parent compounds. Superconductivity in the newly discovered rare-earth iron-based oxide systems ROFeAs (R, rare-earth metal) also arises from either electron[3–7] or hole[8] doping of their non-superconducting parent compounds. The parent material LaOFeAs is metallic but shows anomalies near 150 K in both resistivity and d.c. magnetic susceptibility[3]. Although optical conductivity and theoretical calculations suggest that LaOFeAs exhibits a spin-density-wave (SDW) instability that is suppressed by doping with electrons to induce superconductivity[9], there has been no direct evidence of SDW order. Here we report neutron-scattering experiments that demonstrate that LaOFeAs undergoes an abrupt structural distortion below 155 K, changing the symmetry from tetragonal (space group *P*4/*nmm*) to monoclinic (space group *P*112/*n*) at low temperatures, and then, at ~137 K, develops long-range SDW-type antiferromagnetic order with a small moment but simple magnetic structure[9]. Doping the system with fluorine suppresses both the magnetic order and the structural distortion in favour of superconductivity. Therefore, like high-$T_c$ copper oxides, the superconducting regime in these iron-based materials occurs in close proximity to a long-range-ordered antiferromagnetic ground state.**

The recent discovery of superconductivity in $RO_{1-x}F_xFeAs$ (refs 3–7) has generated enormous interest because these materials are the first non-copper oxide superconductors with $T_c$s exceeding 50 K. Because these superconductors are derived by doping their non-superconducting parent compounds, it is natural to wonder what the ground states of the parent compounds are. It has been argued theoretically that non-superconducting LaOFeAs is either a non-magnetic metal near a magnetic (antiferromagnetic and/or ferromagnetic) instability[10–12] or an antiferromagnetic semimetal[9,13–15]. As a function of temperature, the resistivity of LaOFeAs shows a clear drop around 150 K before increasing again below 50 K (refs 3, 9). The d.c. magnetic susceptibility also has a small anomaly near 150 K. From optical measurements and theoretical calculations[9], it has been argued that LaOFeAs has an antiferromagnetic SDW instability below 150 K and that superconductivity in these materials arises from the suppression of this SDW order.

We used neutron diffraction to study the structural and magnetic order in polycrystalline, non-superconducting LaOFeAs and superconducting $LaO_{1-x}F_xFeAs$ with $x = 0.08$ ($T_c = 26$ K). Our experiments were carried out on the BT-1 powder diffractometer and the BT-7 thermal triple-axis spectrometer at the NIST Center for Neutron Research, and on the HB-1A triple-axis spectrometer at the High Flux Isotope Reactor, Oak Ridge National Laboratory. Figure 1a shows the high-resolution neutron powder diffraction data obtained using the BT-1 diffractometer and our refinements for non-superconducting LaOFeAs at 170 K. Consistent with earlier results[3–9], we find that the crystal structure belongs to the tetragonal space group *P*4/*nmm*, with atomic positions given in Table 1. On cooling the sample to 4 K, the (2, 2, 0) reflection that has a single peak at 170 K (Fig. 1a, inset) is split into two peaks (Fig. 1b, inset). This suggests that a structural phase transition has occurred. For comparison, we note that the (2, 2, 0) peak remains a single peak even at 10 K (Fig. 1c inset) for superconducting $LaO_{0.92}F_{0.08}FeAs$. To understand the low-temperature structural distortion in LaOFeAs, we carried out refinements using the neutron data and found that the structure in fact becomes monoclinic and belongs to space group *P*112/*n* (see Supplementary Information). Table 2 summarizes the low-temperature lattice parameters and atomic positions for LaOFeAs. Table 3 summarizes the lattice parameters and atomic positions for superconducting $LaO_{0.92}F_{0.08}FeAs$ at 10 K, 35 K and 170 K. Figure 1d shows the LaOFeAs structure.

To see if the newly observed structural transition is related to the ~150 K resistivity anomaly, we carried out detailed temperature-dependent measurements of the (2, 2, 0) reflection and found that there is an abrupt splitting of the (2, 2, 0) peak at 155 K (Fig. 2). The peak intensity also shows a clear kink at 155 K. These results indicate that the non-superconducting system has a structural phase transition, and this phase transition is associated with the observed resistivity[3] and specific heat anomalies[9]. Because a similar splitting of the (2, 2, 0) peak is absent in superconducting $LaO_{0.92}F_{0.08}FeAs$ (Fig. 1c), we can safely assume that this transition is suppressed with the

**Table 1 | Properties of LaOFeAs at 175 K**

a, Refined structure parameters

| Atom | Site | *x* | *y* | *z* | *B* (Å$^2$) |
|---|---|---|---|---|---|
| La | 2*c* | ¼ | ¼ | 0.1418(3) | 0.65(7) |
| Fe | 2*b* | ¾ | ¼ | ½ | 0.39(5) |
| As | 2*c* | ¼ | ¼ | 0.6507(4) | 0.23(8) |
| O | 2*a* | ¾ | ¼ | 0 | 0.69(7) |

b, Selected interatomic distances and angles

| | | | |
|---|---|---|---|
| La–As (×4) | 3.378(1) Å | Fe–As (×4) | 2.407(2) Å |
| La–O (×4) | 2.365(2) Å | As–Fe–As | 107.41(7)° |
| Fe–Fe | 2.84969(7) Å | As–Fe–As | 113.7(1)° |

Space group, *P*4/*nmm*; $a = 4.03007(9)$ Å; $c = 8.7368(2)$ Å; $V = 141.898(9)$ Å$^3$. $R_p = 5.24\%$, weighted $R_p = 6.62\%$, $\chi^2 = 0.9821$.

[1]Department of Physics and Astronomy, The University of Tennessee, Knoxville, Tennessee 37996-1200, USA. [2]Oak Ridge National Laboratory, Oak Ridge, Tennessee 37831, USA. [3]NIST Center for Neutron Research, National Institute of Standards and Technology, Gaithersburg, Maryland 20899-6102, USA. [4]Department of Materials Science and Engineering, University of Maryland, College Park, Maryland 20742-6393, USA. [5]Ames Laboratory and Department of Physics and Astronomy, Iowa State University, Ames, Iowa 50011, USA. [6]Beijing National Laboratory for Condensed Matter Physics, Institute of Physics, Chinese Academy of Sciences, Beijing 100080, China.

appearance of superconductivity in $LaO_{1-x}F_xFeAs$ through doping with fluorine.

It would be interesting to see whether this phase transition in non-superconducting LaOFeAs is indeed associated with SDW order. Figure 3a shows our raw data for LaOFeAs collected on the BT-7 spectrometer at 8 K and 170 K. Inspection of the figure immediately reveals that there are extra peaks in the low-temperature spectrum at wavevector magnitudes $Q = 1.15$, 1.53 and 2.5 Å$^{-1}$, which are not

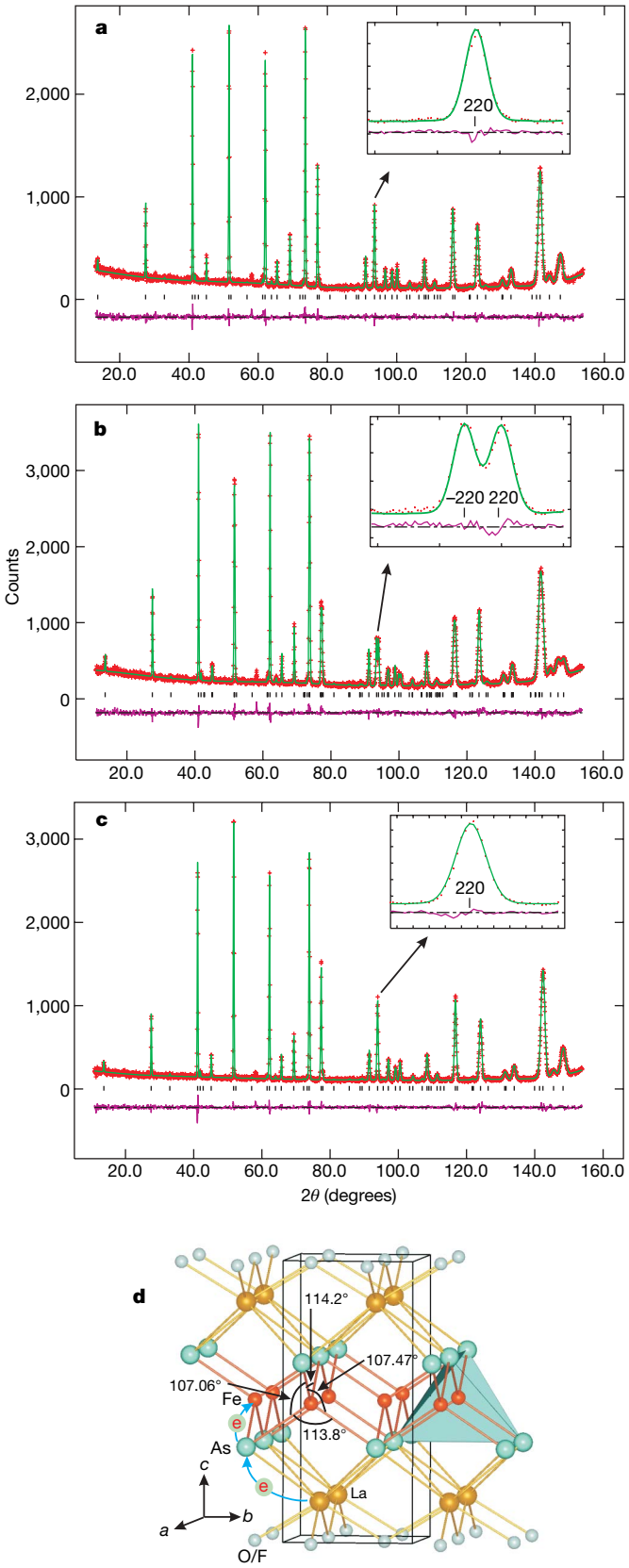


**Figure 1 | Temperature dependence of the nuclear structures for LaOFeAs and $LaO_{0.92}F_{0.08}FeAs$.** We prepared ~2 g each of LaOFeAs and $LaO_{0.92}F_{0.08}FeAs$ using the method described in ref. 9. The BT-1 diffractometer has a Ge(3, 1, 1) monochromator and an incident beam wavelength of $\lambda = 2.0785$ Å. **a**, Observed (red crosses) and calculated (green solid line) neutron powder diffraction intensities of LaOFeAs at 175 K using space group *P*4/*nmm*. The inset shows a single peak of the (2, 2, 0) reflection. Short black vertical lines show the Bragg peak positions. The purple trace indicates the intensity difference between the observed and calculated structures. $\theta$, diffraction angle. **b**, The same scan at 4 K, where the (2, 2, 0) reflection is split owing to the monoclinic distortion. The fit was made using space group *P*112/*n*. **c**, The 10 K scan of superconducting $LaO_{0.92}F_{0.08}FeAs$; the space group *P*4/*nmm* can describe data at all measured temperatures. **d**, Crystal structure of $LaO_{1-x}F_xFeAs$. For $x = 0$, the compound has the charge-balance configuration $La^{3+}O^{2-}Fe^{2+}As^{3-}$. Electron doping can be achieved by replacing O with F.

**Table 2 | Properties of LaOFeAs at 4 K**

a, Refined structure parameters

| Atom | Site | *x* | *y* | *z* | *B* (Å$^2$) |
|---|---|---|---|---|---|
| La | 2*e* | ¼ | ¼ | 0.1426(3) | 0.54(6) |
| Fe | 2*f* | ¾ | ¼ | 0.5006(12) | 0.16(4) |
| As | 2*e* | ¼ | ¼ | 0.6499(4) | 0.23(7) |
| O | 2*f* | ¾ | ¼ | −0.0057(17) | 0.69(7) |

b, Selected interatomic distances and angles

| | | | |
|---|---|---|---|
| La–As (×2) | 3.369(1) Å | Fe–As (×2) | 2.398(6) Å |
| La–As (×2) | 3.380(1) Å | Fe–As (×2) | 2.405(6) Å |
| La–O (×2) | 2.394(8) Å | As–Fe–As | 114.2(5)° |
| La–O (×2) | 2.342(7) Å | As–Fe–As | 107.47(6)° |
| Fe–Fe | 2.8409(2) Å | As–Fe–As | 107.06(6)° |
| Fe–Fe | 2.8548(2) Å | As–Fe–As | 113.8(4)° |

Space group, *P*112/*n*; $a = 4.0275(2)$ Å; $b = 4.0275(2)$ Å; $c = 8.7262(5)$ Å; $\gamma = 90.279(3)°$; $V = 141.54(2)$ Å$^3$. $R_p = 4.31\%$, weighted $R_p = 5.74\%$, $\chi^2 = 1.100$. Lattice constants *a* and *b* were constrained to be equal in the final refinement. For $z(Fe) = 0.5$ and $z(O) = 0$, the structure symmetry can also be described as an orthorhombic structure with *Cmma* space group (see Supplementary Information).

**Table 3 | Properties of $LaO_{0.92}F_{0.08}FeAs$ at 10 K (first line), 35 K (second line) and 175 K (third line)**

a, Refined structure parameters

| Atom | Site | *x* | *y* | *z* | *B* (Å$^2$) |
|---|---|---|---|---|---|
| La | 2*c* | ¼ | ¼ | 0.1448(3) | 0.40(5) |
| | | ¼ | ¼ | 0.1458(3) | 0.50(5) |
| | | ¼ | ¼ | 0.1446(3) | 0.73(5) |
| Fe | 2*b* | ¾ | ¼ | ½ | 0.32(4) |
| | | ¾ | ¼ | ½ | 0.41(4) |
| | | ¾ | ¼ | ½ | 0.65(4) |
| As | 2*c* | ¼ | ¼ | 0.6521(4) | 0.41(7) |
| | | ¼ | ¼ | 0.6515(4) | 0.40(6) |
| | | ¼ | ¼ | 0.6527(4) | 0.69(7) |
| O/F | 2*a* | ¾ | ¼ | 0 | 0.53(6) |
| | | ¾ | ¼ | 0 | 0.62(6) |
| | | ¾ | ¼ | 0 | 0.71(6) |

b, Selected interatomic distances and angles

| | | | |
|---|---|---|---|
| La–As (×4) | 3.347(1) Å | Fe–As (×4) | 2.407(2) Å |
| | 3.345(1) Å | | 2.404(2) Å |
| | 3.349(1) Å | | 2.412(2) Å |
| La–O/F (×4) | 2.373(2) Å | As–Fe–As | 107.61(6)° |
| | 2.377(1) Å | | 107.52(6)° |
| | 2.373(1) Å | | 107.72(6)° |
| Fe–Fe | 2.8427(1) Å | As–Fe–As | 113.3(1)° |
| | 2.8423(1) Å | | 113.5(1)° |
| | 2.8446(1) Å | | 113.0(1)° |

Space group, *P*4/*nmm*. At 10 K, $a = 4.0202(1)$ Å, $c = 8.7034(2)$ Å, $V = 140.66(1)$ Å$^3$, $R_p = 5.34\%$, weighted $R_p = 6.95\%$, $\chi^2 = 1.028$. At 35 K, $a = 4.0196(1)$ Å, $c = 8.7027(2)$ Å, $V = 140.61(1)$ Å$^3$, $R_p = 5.38\%$, weighted $R_p = 6.96\%$, $\chi^2 = 1.050$. At 175 K, $a = 4.0229(1)$ Å, $c = 8.7142(2)$ Å, $V = 141.03(1)$ Å$^3$, $R_p = 5.30\%$, weighted $R_p = 6.93\%$, $\chi^2 = 0.9882$. The small lattice parameter and cell volume differences between 10 K and 35 K data are within the uncertainties of our measurements.

present at 170 K. Indexing these peaks (Fig. 3a) indicates that these reflections are indeed directly related to the nuclear structure and are due to magnetic scattering arising from a simple stripe-type antiferromagnetic structure of iron moments with a magnetic cell $\sqrt{2}a_N \times \sqrt{2}b_N \times 2c_N$ (Fig. 4, top-right inset), where $a_N$, $b_N$, and $c_N$ are the nuclear lattice parameters of the unit cell (see Table 1). Figure 3c shows our refinements considering both the magnetic and structural unit cell. Normalizing the magnetic intensity to the nuclear scattering, we find an ordered iron moment of $0.36(5)\mu_B$ at 8 K (in our results, figures in parentheses indicate uncertainty in the final decimal place; $\mu_B$ denotes the Bohr magneton). For comparison, Fig. 3b shows the HB-1A spectrometer data for LaOFeAs and $LaO_{0.92}F_{0.08}FeAs$. For non-superconducting LaOFeAs, the temperature difference spectrum (8–170 K) shows a clear peak at $Q = 1.53$ Å$^{-1}$, which corresponds to the magnetic (1, 0, 3) Bragg peak. This peak is absent from the scan of superconducting $LaO_{0.92}F_{0.08}FeAs$.

To see if the observed magnetic scattering at low temperature in LaOFeAs is indeed associated with the 150 K phase transition, we carried out order parameter measurements on the strongest (1, 0, 3) magnetic peak using both the BT-7 and the HB-1A spectrometers. Figure 4 shows the temperature dependence of the square of the ordered magnetic moment (normalized at low temperature), which vanishes at ~137 K, about ~18 K lower than the temperature at which the structural phase transition occurs (Fig. 2). Surprisingly, the magnetic order is established at lower temperatures than the structural distortion, much as spin ordering is established after the charge ordering in the static stripe-ordered copper oxide material $La_{1.6-x}Nd_{0.4}Sr_xCuO_4$ with $x = 0.12$ (ref. 16). The presence of the lattice distortion above the Néel temperature is established conclusively in the bottom-left inset of Fig. 4, where a clear lattice distortion is apparent at 138 K. Therefore, the resistivity anomaly at 150 K is caused by the structural distortion, not SDW ordering as originally suggested[9]. The top-right inset in Fig. 4 shows the magnetic structure we determined for the system.

To summarize, we have discovered that the parent compound of the iron-based superconductors is a long-range-ordered antiferromagnet with a simple stripe-type antiferromagnetic structure within the plane that is doubled along the $c$ axis (Fig. 4, top-right inset). There is a structural phase transition before the antiferromagnetic phase transition that changes the structure from space group $P4/nmm$ to space group $P112/n$ at low temperature. The magnetic structure is consistent with the theoretical prediction[9], but the moment of $0.36(5)\mu_B$ per iron atom that we observe at 8 K is much smaller than the predicted value of $\sim 2.3\mu_B$ per iron atom (refs 13, 14). The presence of magnetic frustration might induce the reduced ordered moment[17]. The disappearance of the static antiferromagnetic order and lattice distortion in the doped superconducting materials suggests that the underlying physical properties of this class of superconductors may have important similarities to the high-$T_c$ copper oxides. In any case, we are confident that this new class of materials will open new avenues of research regardless of the origin of the electron pairing and superconductivity.

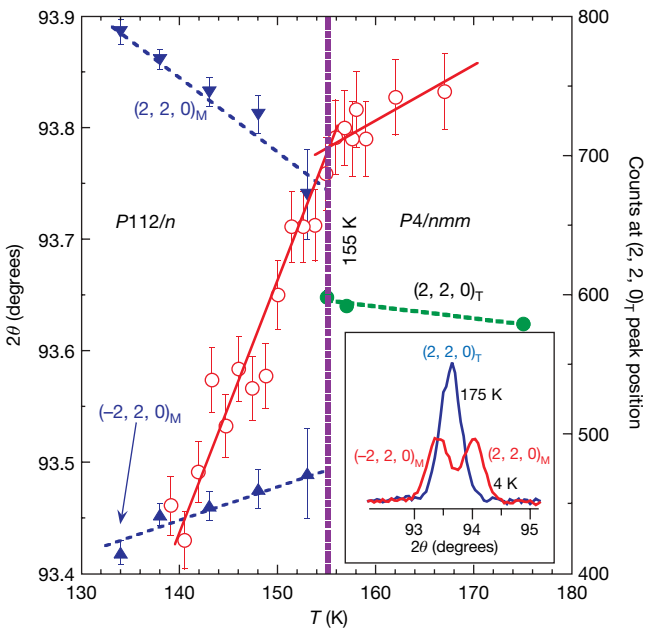


**Figure 2 | Temperature dependence of the (2, 2, 0) nuclear reflection indicative of a structural phase transition at ~155 K in LaOFeAs.** Peak intensities at the $(2, 2, 0)_T$ (tetragonal) reflection (open symbols, right-hand scale) and positions of the $(2, 2, 0)_T$, $(-2, 2, 0)_M$ (monoclinic) and $(2, 2, 0)_M$ peaks (solid symbols, left-hand scale) as a function of temperature on cooling. A structural transition from tetragonal symmetry $P4/nmm$ to monoclinic symmetry $P112/n$ occurs at ~155 K. Error bars, 1 s.d. Inset shows the $(2, 2, 0)_T$ reflection at 175 K and the $(-2, 2, 0)_M$ and $(2, 2, 0)_M$ reflections at 4 K.

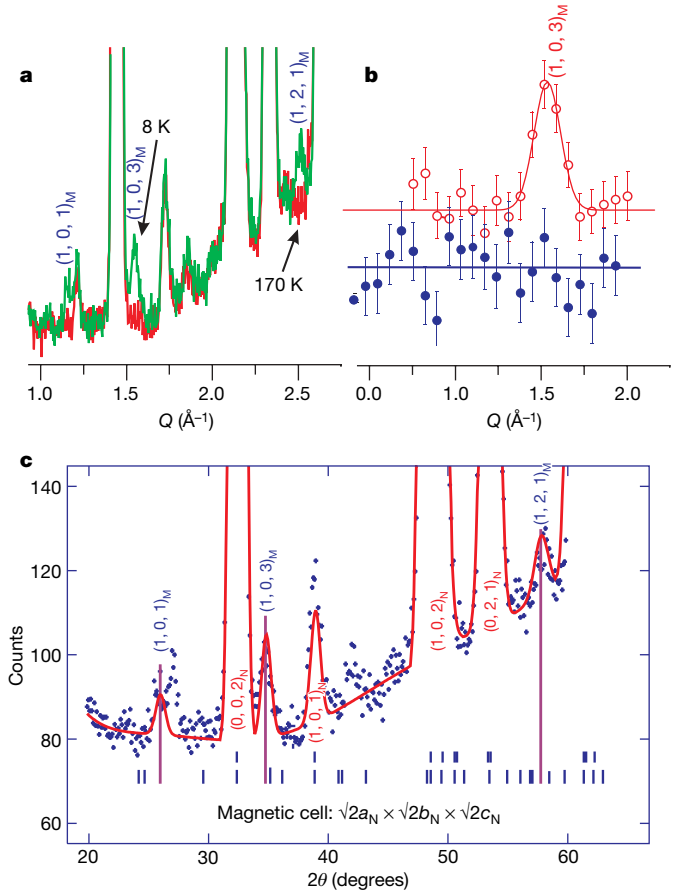


**Figure 3 | Temperature dependence of the magnetic scattering for LaOFeAs and $LaO_{0.92}F_{0.08}FeAs$.** **a**, LaOFeAs data clearly showing (marked) magnetic peaks at 8 K that disappear at 170 K, counting 1 min per point. **b**, The temperature difference spectra (8–170 K) measured using the HB-1A spectrometer for LaOFeAs (red) and $LaO_{0.92}F_{0.08}FeAs$ (blue), counting 4 min per point. The magnetic (1, 0, 3) peak is missing from the $LaO_{0.92}F_{0.08}FeAs$ scan. Error bars, 1 s.d. **c**, LaOFeAs data again showing both magnetic and nuclear Bragg peaks (data, crosses; Bragg peak positions, short vertical lines) together with the model fit (solid line), at 8 K. Data in **a** and **c** were collected using the BT-7 spectrometer with an incident beam wavelength of $\lambda = 2.44$ Å, a PG(0, 0, 2) monochromator and a PG (pyrolytic graphite) filter. Data in **b** were collected using the HB-1A spectrometer with $\lambda = 2.36$ Å and a PG filter.

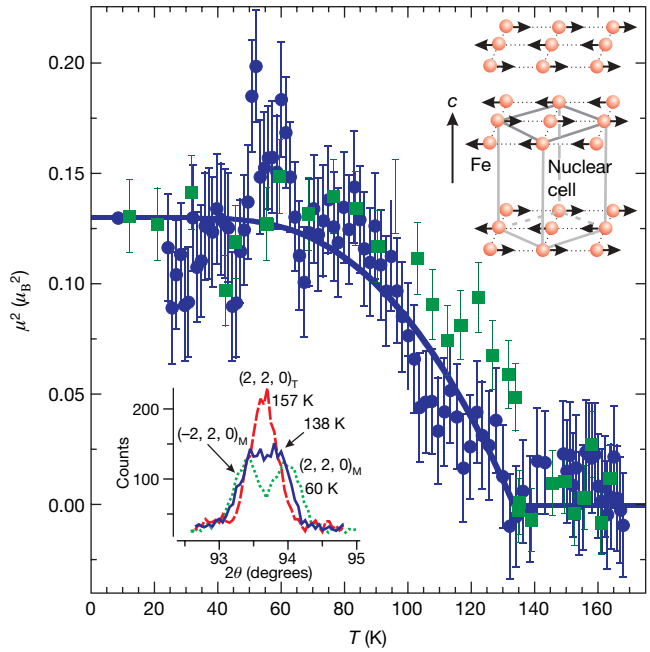


**Figure 4 | Temperature dependence of the order parameter at $Q = 1.53$ Å$^{-1}$, obtained using the magnetic structure we determine for LaOFeAs.** Blue circles, BT-7 spectrometer data; green squares, HB-1A spectrometer data. The solid line is a simple fit to mean field theory that gives a Néel temperature $T_N = 137(3)$ K. The bottom-left inset shows the temperature dependence of the nuclear (2, 2, 0) peak obtained using the BT-1 diffractometer. It is clear that the lattice is distorted at 138 K, before the long-range static antiferromagnetic order sets in at ~137 K. The top-right inset shows the antiferromagnetic structure of the system, giving a $\sqrt{2}a_N \times \sqrt{2}b_N \times 2c_N$ unit cell with moment directions parallel to the planes of iron atoms. To determine the magnetic structure, we note that three magnetic peaks with $h + k + l = 2n$, where $h$, $k$ and $l$ are Miller indices and $n = 0, 1, 2, \ldots$, suggest that the spin configuration has a body-centred symmetry. Our refinements including the spin direction with a $c$-axis component revealed that the $c$ component converged to 0. Because of the very small difference (0.002 Å) in the $a$ and $b$ lattice constants in the orthorhombic magnetic unit cell (see Supplementary Information), it was not possible to determine the spin direction in the $a$–$b$ plane. Error bars, 1 s.d.

**Received 1 April; accepted 2 May 2008.**
**Published online 28 May 2008.**

1. Vaknin, D. *et al.* Antiferromagnetism in $La_2CuO_{4-y}$. *Phys. Rev. Lett.* **58,** 2802–2805 (1987).
2. Tranquada, J. M. *et al.* Neutron-diffraction determination of antiferromagnetic structure of Cu ions in $YBa_2Cu_3O_{6+x}$ with x = 0.0 and 0.15. *Phys. Rev. Lett.* **60,** 156–159 (1988).
3. Kamihara, Y., Watanabe, T., Hirano, M. & Hosono, H. Iron-based layered superconductor La[$O_{1-x}F_x$]FeAs ($x = 0.05$–$0.12$) with $T_c = 26$ K. *J. Am. Chem. Soc.* **130,** 3296–3297 (2008).
4. Chen, G. F. *et al.* Superconducting properties of Fe-based layered superconductor $LaO_{0.9}Fe_{0.1-\delta}FeAs$. Preprint at ⟨http://arxiv.org/abs/0803.0128v1⟩ (2008).
5. Chen, X. H. *et al.* Superconductivity at 43 K in samarium-arsenic oxides SmFeAs$O_{1-x}F_x$. *Nature* advance online publication, doi:10.1038/nature07045 (25 May 2008).
6. Chen, G. F. *et al.* Superconductivity at 41 K and its competition with spin-density-wave instability in layered $CeO_{1-x}Fe_xFeAs$. *Phys. Rev. Lett.* (in the press); preprint at ⟨http://arxiv.org/abs/0803.3790v2⟩ (2008).
7. Ren, Z.-A. *et al.* Superconductivity at 52 K in iron-based F-doped layered quaternary compound Pr[$O_{1-x}F_x$]FeAs. *Mater. Res. Innov.* (in the press); preprint at ⟨http://arxiv.org/abs/0803.4283v1⟩ (2008).
8. Wen, H. H., Mu, G., Fang, L., Yang, H. & Zhu, X. Y. E. Superconductivity at 25 K in hole-doped ($La_{1-x}Sr_x$)OFeAs. *Europhys. Lett.* **82,** 17009 (2008).
9. Dong, J. *et al.* competing orders and spin-density-wave instability in La($O_{1-x}Fe_x$)FeAs. Preprint at ⟨http://arxiv.org/abs/0803.3426v1⟩ (2008).
10. Singh, D. J. & Du, M. H. LaFeAs$O_{1-x}F_x$: A low carrier density superconductor near itinerant magnetism. Preprint at ⟨http://arxiv.org/abs/0803.0429v1⟩ (2008).
11. Xu, G. *et al.* Doping-dependent phase diagram of LaOMAs ($M$ = V–Cu) and electron-type superconductivity near ferromagnetic instability. *Europhys. Lett.* (in the press); preprint at ⟨http://arxiv.org/abs/0803.1282v2⟩ (2008).
12. Haule, K., Shim, J. H. & Kotliar, G. Correlated electronic structure of $LaO_{1-x}F_xFeAs$. *Phys. Rev. Lett.* (in the press); preprint at ⟨http://arxiv.org/abs/0803.1279v1⟩ (2008).
13. Cao, C., Hirschfeld, P. J. & Cheng, H. P. Coexistence of antiferromagnetism with superconductivity in $LaO_{1-x}F_xFeAs$: effective Hamiltonian from ab initio studies. *Phys. Rev. B* (in the press); preprint at ⟨http://arxiv.org/abs/0803.3236v1⟩ (2008).
14. Ma, F. J. & Lu, Z. Y. Iron-based layered superconductor $LaO_{1-x}F_xFeAs$: an antiferromagnetic semimetal. Preprint at ⟨http://arxiv.org/abs/0803.3286v1⟩ (2008).
15. Han, Q., Chen, Y. & Wang, Z. D. A generic two-band model for unconventional superconductivity and spin-density-wave order in electron- and hole-doped iron-based superconductors. *Europhys. Lett.* **82,** 37007 (2008).
16. Tranquada, J. M., Sternlieb, B. J., Axe, J. D., Nakamura, Y. & Uchida, S. Evidence for stripe correlations of spins and holes in copper oxide superconductors. *Nature* **375,** 561–563 (1995).
17. Si, Q. & Abrahams, A. Strong correlations and magnetic frustration in the high $T_c$ iron pnictides. Preprint at ⟨http://arxiv.org/abs/0804.2480v1⟩ (2008).

**Supplementary Information** is linked to the online version of the paper at www.nature.com/nature.

**Acknowledgements** We thank J. A. Fernandez-Baca, H. P. Cheng, T. Yildirim and C. Brown for discussions. This work is supported by the US Department of Energy, Division of Materials Science and Division of Scientific User Facilities, Basic Energy Sciences. This work is also supported by the US Department of Energy through UT/Battelle LLC. The work at the Institute of Physics, Chinese Academy of Sciences, is supported by the Natural Science Foundation of China, the Chinese Academy of Sciences and the Ministry of Science and Technology of China.

**Author Information** Reprints and permissions information is available at www.nature.com/reprints. Correspondence and requests for materials should be addressed to P.D. (daip@ornl.gov).